Metabolically programmed quality control system for dolichol-linked oligosaccharides

Yoichiro Harada[a], Kazuki Nakajima[b,1], Yuki Masahara-Negishi[a], Hudson H. Freeze[c], Takashi Angata[b,2], Naoyuki Taniguchi[d], and Tadashi Suzuki[a,3]

[a]Glycometabolome Team, Systems Glycobiology Research Group and [d]Disease Glycomics Team, Systems Glycobiology Research Group, RIKEN-Max Planck Joint Research Center, Global Research Cluster, RIKEN, 2-1 Hirosawa, Wako, Saitama 351-0198, Japan; [b]Glycorecognition Team, Systems Glycobiology Research Group, RIKEN Advanced Science Institute, 2-1 Hirosawa, Wako, Saitama 351-0198, Japan; and [c]Sanford Children's Health Research Center, Sanford-Burnham Medical Research Institute, La Jolla, CA 92037

Edited by David W. Russell, University of Texas Southwestern Medical Center, Dallas, TX, and approved October 18, 2013 (received for review June 26, 2013)

The glycolipid $Glc_3Man_9GlcNAc_2$-pyrophosphate-dolichol serves as the precursor for asparagine (*N*)-linked protein glycosylation in mammals. The biosynthesis of dolichol-linked oligosaccharides (DLOs) is arrested in low-glucose environments via unknown mechanisms, resulting in abnormal *N*-glycosylation. Here, we show that under glucose deprivation, DLOs are prematurely degraded during the early stages of DLO biosynthesis by pyrophosphatase, leading to the release of singly phosphorylated oligosaccharides into the cytosol. We identified that the level of GDP-mannose (Man), which serves as a donor substrate for DLO biosynthesis, is substantially reduced under glucose deprivation. We provide evidence that the selective shutdown of the GDP-Man biosynthetic pathway is sufficient to induce the release of phosphorylated oligosaccharides. These results indicate that glucose-regulated metabolic changes in the GDP-Man biosynthetic pathway cause the biosynthetic arrest of DLOs and facilitate their premature degradation by pyrophosphatase. We propose that this degradation system may avoid abnormal *N*-glycosylation with premature oligosaccharides under conditions that impair efficient DLO biosynthesis.

In eukaryotes, the biosynthesis of secretory and membrane proteins occurs in the endoplasmic reticulum (ER) (1, 2). Nascent polypeptides emerging from protein-conducting channels into the ER lumen are often cotranslationally modified with oligosaccharides at selected asparagine residues within the consensus sequence N-X-T (X ≠ P) (3). This process, termed *N*-glycosylation, is a fundamental and evolutionarily conserved posttranslational modification that occurs in all domains of life (2, 4). In mammals, *N*-glycosylation requires preassembly of the lipid-linked precursor, which is composed of three glucose (Glc), nine mannose (Man), and two *N*-acetylglucosamine (GlcNAc) residues linked to pyrophosphate (PP)-dolichol (Fig. 1*A*). The monosaccharide units that compose the precursor are donated either directly or indirectly from the nucleotide sugars UDP-Glc, GDP-Man, and UDP-GlcNAc (Fig. 1*B*). Assembly of the precursor is a bipartite process that begins with the synthesis of the $Man_5GlcNAc_2$-PP-dolichol intermediate on the cytosolic side of the ER membrane. The intermediate is transferred with the aid of flippase into the ER lumen (5, 6), where the oligosaccharide assembly pathway synthesizes $Glc_3Man_9GlcNAc_2$-PP-dolichol. The oligosaccharide thus assembled is transferred to nascent polypeptides by oligosaccharyltransferase (OST). The discharged PP-dolichol moiety is dephosphorylated to form monophosphorylated dolichol (P-dolichol), which can serve as an acceptor substrate for the next cycle of oligosaccharide assembly (7–9).

Genetic and environmental factors greatly influence the highly ordered biosynthesis and transfer of dolichol-linked oligosaccharides (DLOs). For instance, genetic mutations in enzymes involved in DLO assembly cause congenital disorders of glycosylation type I (CDG-I) (10), which are a group of inherited disorders characterized by the abnormal accumulation of DLO intermediates. Because mammalian OST preferentially transfers the fully assembled oligosaccharide (11, 12), multiple proteins are hypoglycosylated in CDG-I cases (10). Although the biosynthetic alterations of DLOs in CDG-I have been extensively studied, it remains unclear how abnormally accumulated DLOs are metabolized.

Recently, Peric et al. (13) and Vleugels et al. (14) reported that abnormally accumulated DLO intermediates in CDG-I patient-derived fibroblasts are degraded by an unidentified pyrophosphatase, resulting in the release of singly phosphorylated oligosaccharides (POSs) into the cytosol. Although it has been postulated that the degradation of abnormal DLO intermediates may facilitate the recycling of discharged P-dolichol as the acceptor substrate for DLO biosynthesis, the biological relevance, as well as the molecular basis, for this degradation process remains unclear.

An aberrant *N*-glycosylation process also occurs when mammalian cells are challenged with glucose deprivation (15–18). Pulse-labeling experiments with [2-^{3}H]-mannose indicate that glucose deprivation causes the incomplete assembly of DLOs, resulting in the synthesis of $Man_{2–5}GlcNAc_2$-PP-dolichol as the major intermediate form (15–18) and in the abnormal glycosylation of a

Significance

In mammals, asparagine (*N*)-linked glycosylation of nascent polypeptides synthesized in the endoplasmic reticulum regulates folding, degradation, and intracellular trafficking of the glycoproteins. The normal *N*-glycosylation requires the completely-assembled dolichol-linked oligosaccharide (DLO) as the optimal glycan donor substrate; however, a low-glucose environment causes arrest of the DLO assembly, which results in the synthesis of extensively truncated premature DLOs, thereby increasing a risk of abnormal *N*-glycosylation. Here, we report that under low-glucose conditions, the premature DLOs are efficiently degraded by unidentified pyrophosphatase, catabolizing them to singly phosphorylated oligosaccharides. Our results suggest that the pyrophosphatase-mediated degradation of premature DLOs functions as a quality control system to avoid abnormal *N*-glycosylation under conditions that impair efficient DLO biosynthesis.

Author contributions: Y.H. and T.S. designed research; Y.H. and K.N. performed research; Y.H. and Y.M.-N. contributed new reagents/analytic tools; Y.H., K.N., H.H.F., T.A., N.T., and T.S. analyzed data; and Y.H., K.N., H.H.F., T.A., N.T., and T.S. wrote the paper.

The authors declare no conflict of interest.

This article is a PNAS Direct Submission.

[1]Present address: Molecular Membrane Neuroscience, RIKEN Brain Science Institute, 2-1 Hirosawa, Wako, Saitama 351-0198, Japan.

[2]Present address: Institute of Biological Chemistry, Academia Sinica, Nankang, Taipei 115, Taiwan.

[3]To whom correspondence should be addressed. E-mail: tsuzuki_gm@riken.jp.

This article contains supporting information online at www.pnas.org/lookup/suppl/doi:10.1073/pnas.1312187110/-/DCSupplemental.

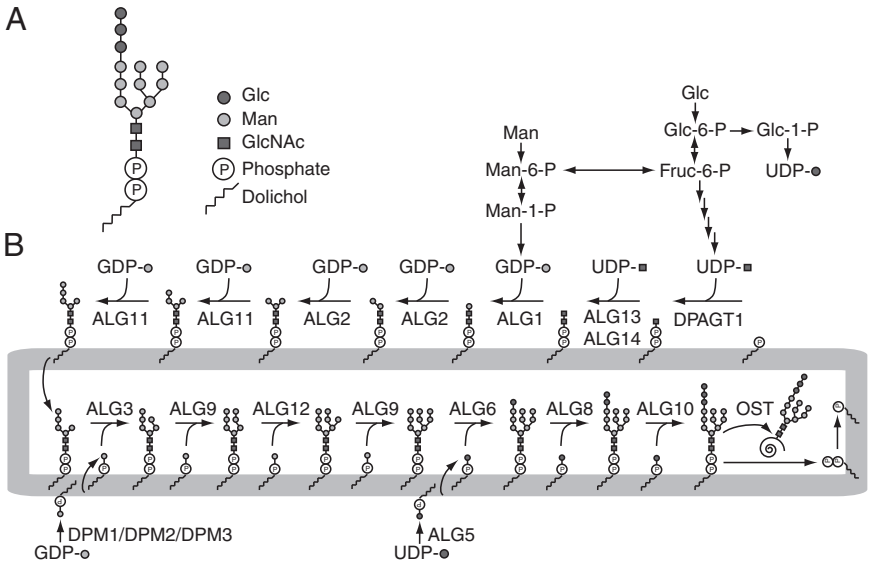

Fig. 1. Model for *N*-glycoprotein biosynthesis in mammals. (*A*) Structure of fully assembled $Glc_3Man_9GlcNAc_2$-PP-dolichol. (*B*) Model for the biosynthetic pathway and transfer of DLOs to proteins. Fruc-6-P, fructose 6-phosphate; Glc-1-P, glucose 1-phosphate; Glc-6-P, glucose 6-phosphate; Man-1-P, mannose 1-phosphate; Man-6-P, mannose 6-phosphate.

subset of glycoproteins (19). However, it remains largely unknown how glucose availability controls the biosynthesis of DLOs.

In the present study, we attempted to elucidate the molecular mechanism underlying the glucose-regulated biosynthesis of DLOs by characterizing the structures of DLO metabolites formed in mouse embryonic fibroblasts (MEFs) under glucose-deprived conditions.

Results

Low-Glucose Conditions Lead to the Loss of DLOs. To elucidate the molecular mechanism underlying the control of DLO biosynthesis by glucose availability, we analyzed the amount and oligosaccharide structures of DLOs accumulated in nondeprived and glucose-deprived MEFs. MEFs, which were preincubated for 24 h under high-glucose conditions (25 mM Glc; Fig. 2*A*), were further cultured for 24 h under normal-glucose (5 mM Glc; Fig. 2*A*) or low-glucose (0.5 mM Glc; Fig. 2*A*) conditions before DLO extraction. The oligosaccharide moieties of DLOs extracted from cells cultured under the two conditions were labeled with 2-aminopyridine (PA) after mild acid hydrolysis, and then analyzed by size-fractionation HPLC. In the normal-glucose environment, fully assembled $Glc_3Man_9GlcNAc_2$-PP-dolichol was prominent and DLO intermediates only accumulated at low levels (Fig. 2*B*). In contrast, the amount of $Glc_3Man_9GlcNAc_2$-PP-dolichol detected in glucose-deprived MEFs was markedly reduced. Notably, no DLO intermediates, except for a trace amount of $Man_2GlcNAc_2$-PP-dolichol, accumulated under low-glucose conditions (Fig. 2*B*). As shown in Fig. 2 *C* and *D*, the amounts of $Glc_3Man_9GlcNAc_2$-PP-dolichol gradually decreased over the 24-h culture period under low-glucose conditions. In addition, trace amounts of $Man_2GlcNAc_2$-PP-dolichol, as well as $Man_{5-7}GlcNAc_2$-PP-dolichol, were detected at 12 h (Fig. 2*C*). Although $Man_{5-7}GlcNAc_2$-PP-dolichol was undetectable after 18 h, $Man_2GlcNAc_2$-PP-dolichol was continuously detected, albeit in trace amounts, even after 24 h of incubation under low-glucose conditions (Fig. 2*C*). Collectively, this result indicated that the exposure of MEFs to low-glucose conditions leads to a dramatic loss of DLOs.

DLO Intermediates Synthesized Under Low-Glucose Conditions Are Prematurely Degraded. To understand the mechanism underlying the loss of DLOs under low-glucose conditions better, we focused on two distinct DLO degradation pathways that involve cleavage at either the GlcNAc-phosphate bond of DLOs to generate free neutral oligosaccharides (20, 21) or the pyrophosphate bond to generate POSs (13, 14, 22). Structural analysis and quantification of the free neutral oligosaccharides in MEFs cultured under normal- and low-glucose conditions did not reveal any remarkable differences (Fig. S1). We therefore examined if POSs were generated under low-glucose conditions. To identify and quantitate POSs unambiguously, we adapted a conventional fluorescent labeling technique to label POSs at their reducing ends after dephosphorylation by treatment with recombinant calf intestine alkaline phosphatase (CIP). This

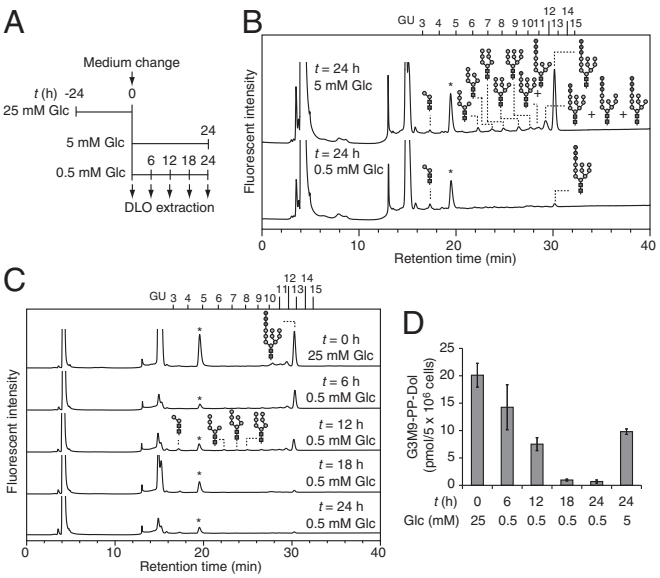

Fig. 2. Low-glucose conditions lead to the loss of DLOs. (*A*) Schematic diagram for cell cultivation. (*B*) Size-fractionation HPLC profiles of DLOs prepared from MEFs incubated for 24 h under normal-glucose (t = 24 h, 5 mM Glc) and low-glucose (t = 24 h, 0.5 mM Glc) conditions. (*C*) Time course analysis of DLO levels under low-glucose conditions. Elution positions of the glucose oligomer [degree of polymerization (DP) = 3–15] are indicated as glucose unit (GU) above the HPLC chart. Asterisks indicate the nonspecific peaks derived from the labeling reagents. (*D*) Quantitation of $Glc_3Man_9GlcNAc_2$-PP-dolichol (G3M9-PP-Dol) in MEFs under high-glucose (t = 0 h, 25 mMGlc), low-glucose (t = 6–24 h, 0.5 mM Glc), and normal-glucose (t = 24 h, 5 mM Glc) conditions. Error bars indicate SDs from three independent experiments.

method allowed for the specific detection of POSs, which can only be labeled when the phosphate group is removed by CIP.

POSs were isolated from MEFs cultured under normal- and low-glucose conditions by enriching for acidic oligosaccharides in the soluble oligosaccharide fraction using anion-exchange chromatography. The CIP-treated POSs were labeled with PA at the liberated reducing end of the oligosaccharides and then analyzed by HPLC. As shown in Fig. 3*A*, eight peaks (a–h) were unique to the CIP-treated POSs. Of those, three peaks (a–c in Fig. 3 *A* and *B*) were markedly increased under low-glucose conditions, whereas the other five peaks (d–h in Fig. 3 *A* and *B*) changed only minimally between the two glucose conditions. Among the eight detected peaks, six peaks (c–h in Fig. 3*A*) were reduced following the α-mannosidase treatment of labeled POSs (Fig. S2*A*), suggesting that the α-mannosidase–sensitive peaks are structurally related to high-mannose type glycans.

To determine the isomeric glycan structures of peaks a–h (Fig. 3*A*), the corresponding POSs were analyzed in parallel with a series of standard PA-labeled glycans (Table S1) by dual-gradient, reversed-phase HPLC (23). Based on their elution positions, the glycan structures of the oligosaccharides corresponding to peaks a–h were determined to be Gn2, M1A, M2A, M3B, M4D, M5B, M6E, and M7E, respectively (Fig. 3*A* and Table S1). All identified oligosaccharide structures were identical to those found in DLO intermediates (Fig. 1*B*).

Although we identified several phosphorylated high-mannose type glycans in MEFs, it was not clear whether they were structurally identical to previously characterized POSs in CDG-I patient-derived fibroblasts (13, 14), because the number of terminal phosphate groups was not determined. To investigate whether the high-mannose type glycans detected in MEFs were mono- or diphosphorylated, the acidic oligosaccharide fraction was subjected to anion-exchange chromatography and eluted with varying concentrations of NaCl. Phosphorylated glycans in the sample were eluted with between 20 and 70 mM NaCl, and coeluted with the monophosphorylated compound AMP but not with diphosphorylated ADP (Fig. S2*B*). All these results indicated that the overall structures of the phosphorylated high-mannose type glycans were determined to be $Man_{0–7}GlcNAc_2$-Ps, which are identical to POSs found in CDG-I patient-derived fibroblasts (13, 14).

To determine the subcellular localization of POSs, we permeabilized the plasma membrane of glucose-deprived MEFs with 0.02% digitonin and obtained cytosol and membrane fractions by centrifugation. The membrane integrity of the lysosome and the ER was confirmed by recovery of the lysosome marker β-hexosaminidase (Fig. S2*C*) and the ER marker protein disulfide isomerase in the membrane fraction (Fig. S2*D*). The cytosol fraction was found to contain over 85% of the cytosolic protein GAPDH (Fig. S2*E*), indicating that the specific permeabilization of the plasma membrane was successful. We found that POSs were exclusively recovered in the cytosol fraction (Fig. S2*F*). Together, these biochemical characterizations strongly indicated that the POSs were generated from DLO intermediates through the action of an unidentified pyrophosphatase (13, 14). Importantly, the quantitative analysis of POSs showed that under low-glucose conditions, the small species of POSs, particularly $Man_{0–2}GlcNAc_2$-Ps, substantially accumulated in a time-dependent manner (Fig. 3*C*). This result indicated that the release of $Man_{0–2}GlcNAc_2$-Ps from DLOs was induced in MEFs cultured under low-glucose conditions.

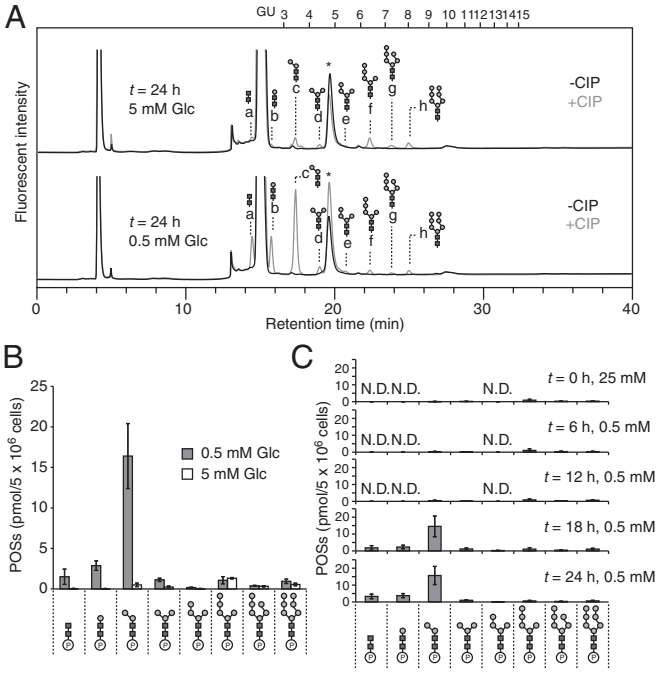

Fig. 3. Low-glucose conditions induce the release of POSs from $Man_{0–2}GlcNAc_2$-PP-dolichol. (*A*) Size-fractionation HPLC profiles of POSs prepared from MEFs cultured for 24 h under normal-glucose (t = 24 h, 5 mM Glc) and low-glucose (t = 24 h, 0.5 mM Glc) conditions. An acidic oligosaccharide fraction enriched by anion-exchange chromatography was treated with (+) or without (–) CIP, followed by fluorescent labeling with PA. Peaks a–h were specifically detected by the CIP treatment. Elution positions of the glucose oligomer (DP = 3–15) are indicated above the HPLC chart. Asterisks indicate the nonspecific peaks derived from the labeling reagents. (*B*) Quantitation of the POSs in *A*. Gray bars, low-glucose conditions (0.5 mM Glc); white bars, normal-glucose conditions (5 mM Glc). (*C*) Time course analysis of POS levels under low-glucose conditions. N.D., not detected. Error bars indicate SDs from three independent experiments.

Unfolded Protein Response Does Not Induce the Release of POSs. Although our experimental findings clearly demonstrated that low-glucose conditions induced the release of POSs from DLO intermediates, the critical factor(s) regulating this process remained unclear. Because it has been well documented that low-glucose conditions activate the unfolded protein response (UPR) (24, 25), we performed a time course analysis of UPR activation in MEFs to determine if the UPR is associated with the release of POSs. Under low-glucose conditions, the UPR was strongly activated at 18 h, as judged by the transcriptional up-regulation of a UPR marker, glucose-regulated protein 78/ immunoglobulin heavy chain-binding protein (24, 25) (Fig. S3*A*). As shown in Fig. 3*B*, the accumulation of $Man_{0–2}GlcNAc_2$-Ps coincided with UPR activation. Accordingly, we examined whether the UPR is directly involved in the release of POSs from DLO, even under normal-glucose conditions. To this end, MEFs were treated for 6 h with DTT, a well-characterized UPR inducer, under normal-glucose conditions. Although the UPR was strongly activated by the DTT treatment (Fig. S3*B*), $Man_{0–2}GlcNAc_2$-Ps were not detected.

UPR is known to activate the interferon-inducible RNA-dependent protein kinase (PKR)-like ER kinase (PERK) signaling pathway, which attenuates global translation (26). As a consequence, loading of proteins harboring *N*-glycosylation acceptor sites into the ER lumen is reduced, leading to the accumulation of excess DLOs. To test whether translation inhibition triggers the degradation of accumulated DLOs by pyrophosphatase, WT MEFs were treated with cycloheximide (CHX), a translation inhibitor, under normal-glucose conditions. However, we found that POS release was not induced by CHX treatment. We next examined POSs accumulated in $PERK^{-/-}$ MEFs cultured under low-glucose conditions to determine if a failure in the UPR-induced translational attenuation inhibits POS release. In the preculture conditions (Fig. S3*C*; t = 0 h, 25 mM Glc), almost no $Man_{0–2}GlcNAc_2$-Ps was detected. However, after 18 h of glucose

deprivation, $Man_{0–2}GlcNAc_2$-Ps had clearly accumulated (Fig. S3*C*), further suggesting that PERK-dependent translation attenuation is not critical for the formation of POSs. Collectively, these results strongly indicated that neither UPR nor translation arrest is a critical factor for inducing the release of POSs.

Glucose Availability Regulates Nucleotide Sugar Levels. The intracellular pool of the nucleotide sugars UDP-GlcNAc, GDP-Man, and UDP-Glc, which are essential precursors for the biosynthesis of DLOs, is regulated by glucose metabolism (27). To examine whether a correlation exists between the release of POSs and nucleotide sugar levels under low-glucose conditions, the amounts of UDP-GlcNAc, GDP-Man, and UDP-Glc were quantitated at various time points in MEFs shifted from high-glucose to low-glucose conditions. Under low-glucose conditions, the level of UDP-GlcNAc, which is required for the synthesis of the *N,N′*-diacetylchitobiosyl core structure of DLOs, was reduced to levels comparable to those under normal-glucose conditions after 18 h, with the level remaining constant until 24 h (Fig. 4*A*). In contrast, the levels of GDP-Man (Fig. 4*B*) and UDP-Glc (Fig. 4*C*) gradually reduced and were almost undetectable after 18 h. Notably, the depletion of GDP-Man and UDP-Glc coincided with the induced release of $Man_{0–2}GlcNAc_2$-Ps (Fig. 3*B*). This observation led us to hypothesize that the substantial reduction of these two nucleotide sugars results in the maturation arrest of DLOs, which may, in turn, induce the release of POSs from DLO intermediates.

GDP-Man Biosynthetic Pathway Regulates the Release of POSs from DLO Intermediates. Because $Man_{0–2}GlcNAc_2$-PP-dolichol underwent the release of POSs without acquiring the third mannose residue (Fig. 1*B*), we hypothesized that the level of GDP-Man, which serves as the mannose donor substrate, is more critical to regulate the release of POSs. To analyze the role of the GDP-Man biosynthetic pathway in the regulated release of POSs, we quantitated the levels of GDP-Man in mannose 6-phosphate isomerase (MPI)-KO MEFs ($MPI^{-/-}$ MEFs) (28). Under physiological conditions, GDP-Man is predominantly synthesized from glucose (29) through the interconversion of fructose 6-phosphate to mannose 6-phosphate by MPI (Fig. 1*B*). Because $MPI^{-/-}$ MEFs are devoid of this interconversion pathway, GDP-Man biosynthesis in these cells is exclusively dependent upon the supply of mannose (28, 30), providing an ideal system to modulate the GDP-Man biosynthetic pathway without altering the glucose supply. Mannose can be taken up from culture medium and/or salvaged from the degradation of mannose-containing glycoconjugates by class II α-mannosidases (28, 30). Accordingly, to shut down the mannose utilization pathway in $MPI^{-/-}$ MEFs, the cells were incubated in medium supplemented with 5 mM glucose, 10% (vol/vol) dialyzed FBS, and 10 μM class II α-mannosidase inhibitor swainsonine (SW) (28, 30). After only 6 h of mannose deprivation, the level of GDP-Man was significantly reduced, and it was further decreased up to 18 h (Fig. 5*A*, *Top*). Importantly, normal GDP-Man biosynthesis was restored by mannose replenishment (Fig. 5*A*, *Top*), confirming that mannose utilization is crucial for GDP-Man biosynthesis in $MPI^{-/-}$ MEFs. Interestingly, UDP-Glc (Fig. 5*A*, *Middle*) and UDP-GlcNAc (Fig. 5*A*, *Bottom*) were unexpectedly increased by mannose deprivation through a yet unknown mechanism.

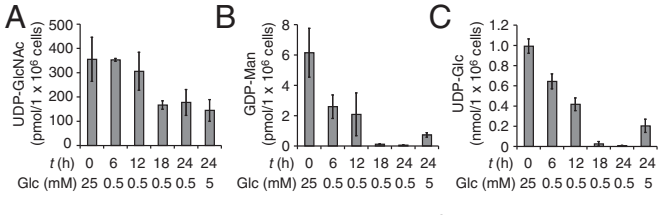

Fig. 4. Glucose availability regulates the levels of nucleotide sugars. MEFs that were precultured under high-glucose conditions (t = 0 h, 25 mM) were further incubated for the indicated time under either low-glucose (0.5 mM Glc) or normal-glucose (5 mM Glc) conditions, and UDP-GlcNAc (*A*), GDP-Man (*B*), and UDP-Glc (*C*) were quantitated by ion-paired, reversed-phase HPLC. Error bars indicate SDs from three independent experiments.

When $MPI^{-/-}$ MEFs were maintained in medium supplemented with 20 μM mannose, similar amounts of $Glc_3Man_9GlcNAc_2$-PP-dolichol and $Man_5GlcNAc_2$-PP-dolichol accumulated in the cells (Fig. 5*B*, *Top* and *Middle*). After 6 h of mannose deprivation, the two DLO species were barely detected. Furthermore, mannose deprivation resulted in a slight increase in $Man_2GlcNAc_2$-PP-dolichol levels (Fig. 5*B*, *Bottom*). We confirmed that the defects in DLO biosynthesis were fully restored by mannose replenishment (Fig. 5*B*, *Top*). In a control experiment, we also showed that DLO biosynthesis in WT MEFs was not affected by mannose deprivation (Fig. S4*A*).

Having confirmed the mannose dependency of DLO biosynthesis in $MPI^{-/-}$ MEFs, we next examined the release of POSs in $MPI^{-/-}$ MEFs under conditions of mannose deprivation. When $MPI^{-/-}$ MEFs were cultured in the presence of mannose, three POS species, including $Man_{2,5,7}GlcNAc_2$-Ps, were detected as the major forms (Fig. 5*C*). In contrast, upon mannose deprivation, $Man_2GlcNAc_2$-P specifically accumulated in a time-dependent manner (Fig. 5*C*, *Top*), whereas $Man_{5,7}GlcNAc_2$-Ps were gradually reduced (Fig. 5*C*, *Middle* and *Bottom*). WT MEFs did not accumulate $Man_2GlcNAc_2$-P under the same conditions (Fig. S4*B*). These results showed that in $MPI^{-/-}$ MEFs, mannose deprivation is sufficient to induce the selective degradation of $Man_2GlcNAc_2$-PP-dolichol even under a physiological Glc concentration.

Discussion

In the present study, we demonstrated that low-glucose conditions induce the premature degradation of DLOs and release of POSs. We also showed that the GDP-Man biosynthetic pathway is the key regulator for the degradation of DLO intermediates. These findings shed light on the regulatory mechanism used to maintain the quality of DLOs under conditions that impair efficient DLO biosynthesis.

Our biochemical analysis of DLOs showed that although the intracellular levels of fully assembled $Glc_3Man_9GlcNAc_2$-PP-dolichol gradually decrease under low-glucose conditions, DLO intermediates accumulate at only low levels. This result contrasts with previous findings from pulse labeling experiments with [2-^{3}H]-mannose, showing that DLO intermediates clearly accumulate during glucose deprivation (15–18). The apparent discrepancy between these studies may be due to the fact that DLOs were analyzed during the pulse-labeling period, and therefore does not necessarily reflect the steady-state level of DLOs. The $t_{1/2}$ of [2-^{3}H]-mannose–labeled DLO in mammalian cells is estimated to be ∼15 min (29).

The structure of the most abundant POS in MEFs was revealed to be $Man_2GlcNAc_2$-P, whose oligosaccharide structure is synthesized by the bifunctional α-mannosyltransferase ALG2 (Fig. 1*B*). This enzyme synthesizes $Man_3GlcNAc_2$-PP-dolichol by the successive addition of α1,3- and α1,6-linked mannose residues from GDP-Man to $Man_1GlcNAc_2$-PP-dolichol (31–33). The first reaction catalyzed by ALG2 preferentially forms the α1,3-linked mannose branch of $Man_2GlcNAc_2$-PP-dolichol (31–33). We showed that $Man_2GlcNAc_2$-P is solely composed of the same glycan conformer as $Man_2GlcNAc_2$-PP-dolichol, indicating that the second step of the ALG2 reaction is arrested under glucose deprivation. Although it remains to be determined how such regulation is achieved, the fact that a substantial reduction of GDP-Man occurs under low-glucose conditions raises the possibility that the second ALG2 reaction may have a higher K_m value for GDP-Man than the first reaction. It should be noted

BIOCHEMISTRY

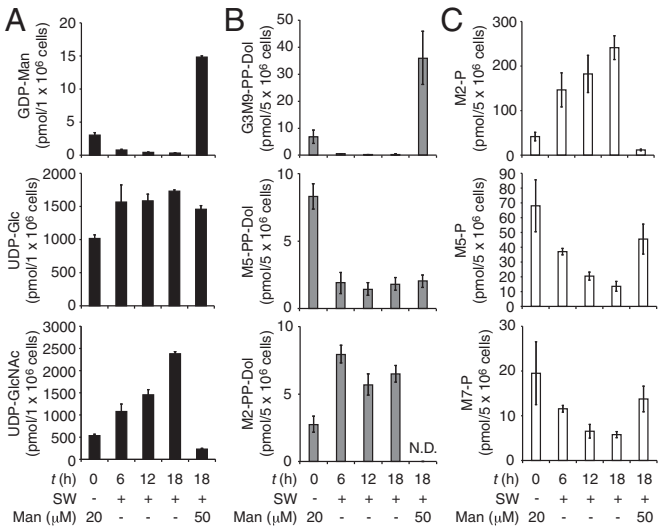

Fig. 5. Shutdown of the GDP-Man biosynthetic pathway in MPI$^{-/-}$ MEFs induces the release of POS from $Man_2GlcNAc_2$-PP-dolichol. A time course analysis of nucleotide sugars (*A*), DLOs (*B*), and POSs (*C*) in MPI$^{-/-}$ MEFs was performed. Cells maintained in culture medium supplemented with 25 mM Glc, 20% (vol/vol) FBS, and 20 μM Man (0 h) were shifted to medium supplemented with 5 mM Glc and 10% (vol/vol) dialyzed FBS, which was further supplemented with (+) or without (–) 10 μM SW and 50 μM Man (18 h). Error bars indicate SDs from three independent experiments. N.D., not detected. G3M9-PP-Dol, $Glc_3Man_9GlcNAc_2$-PP-dolichol; M2-P, $Man_2GlcNAc_2$-P; M5-P, $Man_5GlcNAc_2$-P; M7-P, $Man_7GlcNAc_2$-P; M2-PP-Dol, $Man_2GlcNAc_2$-PP-dolichol; M5-PP-Dol, $Man_5GlcNAc_2$-PP-dolichol.

that the synthesis of $Man_1GlcNAc_2$-PP-dolichol by ALG1 is prerequisite for the ALG2 reaction to proceed (Fig. 1*B*). Based on our POS analysis, it appears that the activity of ALG1 is not severely affected under low-glucose conditions, implying that ALG1 may have a low K_m value for GDP-Man. These biosynthetic regulations of DLOs may be involved in the preferential degradation of $Man_2GlcNAc_2$-PP-dolichol under low-glucose conditions, thereby eliminating the aberrant DLO intermediates that fail to be completely assembled into $Glc_3Man_9GlcNAc_2$-PP-dolichol.

Our results raise the question of why mammalian cells degrade DLO intermediates when oligosaccharide assembly is impaired. During maturation of glycoproteins in the secretory pathway, *N*-glycans undergo drastic structural remodeling by the action of various luminal glycosidases and glycosyltransferases (34), which play central roles in folding, degradation, intracellular trafficking, and functional regulation of the glycoproteins (1, 34). The transfer of extensively truncated glycans, such as $Man_2GlcNAc_2$ synthesized under low-glucose conditions, onto nascent polypeptides would prevent their correct structural remodeling, leading to the dysregulation of these biologically important processes. It is therefore possible that the degradation of DLO intermediates in a metabolic deficiency may function as a quality control system to avoid abnormal *N*-glycosylation, thereby protecting cells from the accumulation of nonfunctional glycoproteins. However, in the case of ALG2-CDG fibroblasts, $Man_{1-2}GlcNAc_2$-PP-dolichol is constitutively accumulated (31) and only minimally transferred onto proteins (31). However, these truncated glycans are metabolized to POSs (14), resulting in a reduced level of fully assembled DLO and hypoglycosylation of transferrin (31).

The formation of POSs from both the cytosolic and luminal species of DLO intermediates, particularly $Man_{0-7}GlcNAc_2$-PP-dolichol, raises a topological issue concerning DLO degradation. Using a reconstituted lipid bilayer, it was demonstrated that the DLO flippase enables the bidirectional movement of DLOs with various oligosaccharide structures in the ER (6). This is also true in mammalian cultured cells, because $GlcNAc_2$-PP-dolichol synthesized on the cytosolic side of the ER membrane is transferred to proteins (19). Therefore, the degradation of DLO intermediates (13, 14) can theoretically occur on either side of the ER membrane. It is also possible that two or more distinct pyrophosphatases exist on both sides of the ER membrane. Regardless of the exact mechanism, our analyses clearly demonstrate that the POSs released from DLO intermediates extensively accumulate in the cytosol. Identification and biochemical characterization of the DLO pyrophosphatase are necessary to determine conclusively the site where the pyrophosphatase reacts with DLOs.

To ensure the proper maturation of DLOs, their degradation must be strictly regulated under normal conditions. The metabolically programmed degradation system of DLOs enables cells not only to avoid unnecessary DLO degradation but to regulate both the quality and quantity of DLOs rapidly and reversibly in response to environmental changes. To obtain a better understanding of the molecular mechanism underlying the DLO degradation process, the precise targets of the GDP-Man biosynthetic pathway, as well as the nature of the DLO pyrophosphatase, need to be clarified in future studies.

Materials and Methods

Preparation of MEFs. MEFs were established from the fetuses of WT B6 mice. The detailed methods are provided in *SI Materials and Methods*. All experimental protocols and procedures were approved by the Ethical Committees on Animal Research of RIKEN.

Cell Culture. MEFs established in this study were maintained in complete DMEM containing 25 mM Glc, 10% (vol/vol) FBS, 100 U/mL penicillin, and 100 μg/mL streptomycin (high-glucose conditions). The previously established MPI$^{-/-}$ MEFs and the WT MEFs (control) (28) were maintained in mannose-supplemented DMEM containing 25 mM Glc, 20 μM Man, 20% (vol/vol) FBS, 100 U/mL penicillin, and 100 μg/mL streptomycin. PERK$^{-/-}$ MEFs (35) were a generous gift from David Ron (University of Cambridge, Cambridge, United Kingdom) and were maintained in the high-glucose medium supplemented with 1× nonessential amino acids (Invitrogen) and 55 μM β-mercaptoethanol (Invitrogen), and the medium was changed every 24 h. All cells were cultivated at 37 °C in a 5% (vol/vol) CO_2 atmosphere.

Cultivation of MEFs Under Normal- and Low-Glucose Conditions. MEFs (2×10^6 cells) were cultured in 15-cm dishes containing 20 mL of DMEM (high-glucose conditions) for 24 h at 37 °C. The cells were washed twice with 10 mL of DMEM without glucose (Invitrogen) and then further incubated for 24 h at 37 °C in 20 mL of DMEM without glucose supplemented with 10% (vol/vol) FBS, 100 U/mL penicillin, 100 μg/mL streptomycin, and either 5 mM Glc (normal-glucose conditions) or 0.5 mM Glc (low-glucose conditions). In the case of experiments using PERK$^{-/-}$ MEFs, medium was supplemented with 1× nonessential amino acids and 55 μM β-mercaptoethanol. For time course experiments, cells for $t = 0$ h were harvested just after the 24-h preculture under high-glucose (25 mM Glc) conditions without changing the culture medium.

Mannose Deprivation. MPI$^{-/-}$ MEFs and the WT control MEFs (0.5×10^6 cells) were cultured for 24 h in 10-cm dishes containing 10 mL of mannose-supplemented DMEM. The cells were washed twice with 5 mL of DMEM without glucose and then incubated for the indicated time in 10 mL of DMEM without glucose supplemented with or without 50 μM mannose, and with 5 mM Glc, 10% (vol/vol) dialyzed FBS (Gibco), 100 U/mL penicillin, 100 μg/mL streptomycin, and 10 μM SW (Wako Pure Chemical Industries).

Preparation of DLOs. For the preparation of DLOs, MEFs were extracted with 75% (vol/vol) ice-cold ethanol. The resulting suspension was centrifuged at 15,000 × *g* for 15 min at 4 °C, and the cell pellet was then washed twice with 5 mL of methanol. The pellet was extracted twice with 4 mL of chloroform/methanol (2:1, vol/vol) and dried. The dried pellet was further extracted twice with 4 mL of methanol/water (1:1, vol/vol) containing 4 mM $MgCl_2$. DLOs were then extracted from the pellet twice with 4 mL of chloroform/methanol/water (10:10:3, vol/vol/vol). After the DLO fraction was evaporated to dryness, the residual pellet was heated for 30 min at 100 °C in 1 mL of 20 mM HCl containing 50% (vol/vol) isopropanol. The reaction mixture was

evaporated to dryness and resuspended in 1 mL of water. The water-soluble fraction containing the released oligosaccharides was desalted using an InertSep GC column, followed by a coupled-ion exchange column (AG1-X2 acetate form and AG50-X8 H^+ form).

Preparation of POSs. To prepare POSs, MEFs were extracted with 75% (vol/vol) ice-cold ethanol, and the soluble fraction was evaporated to dryness. The dried pellet was resuspended in 2 mL of water and desalted using a PD-10 column (GE Healthcare) equilibrated with 5% (vol/vol) ethanol. The desalted sample was adjusted to 10 mM Tris·HCl (pH 7.4) and then passed through a Sep-Pak Accell QMA column (Waters) that had been washed with 5 mL of 1 M NaCl, followed by 20 mL of 10 mM Tris·HCl (pH 7.4). The flow-through fraction was discarded, and the column was washed with 20 mL of 10 mM Tris·HCl (pH 7.4). The bound materials were eluted with 5 mL of buffer containing 10 mM Tris·HCl (pH 7.4) and 70 mM NaCl. The eluate was saved as the acidic oligosaccharide fraction and divided equally into two samples. Recombinant CIP (1 U; Roche) was added to one sample, and the other sample was left untreated. After incubation of the two samples for 16 h at 37 °C, the reaction was stopped by heating for 5 min at 80 °C and the samples were desalted as described in the previous section on preparation of DLOs.

Pyridylamination. Fluorescent labeling of soluble oligosaccharides with PA (Wako Pure Chemical Industries) was performed as described previously (36–38).

HPLC. Size-fractionation HPLC (38) and dual-gradient, reversed-phase HPLC (23) were performed as described previously. Each PA-labeled glycan was quantitated based on fluorescent intensity of PA-labeled isomaltohexaose in the standard PA-labeled glucose oligomer (degree of polymerization = 3–15; Takara).

Analysis of Nucleotide Sugars by Ion-Pair Reversed-Phase HPLC and Liquid Chromatography-MS/MS. The amounts of GDP-Man, UDP-Glc, and UDP-GlcNAc were simultaneously measured in samples by HPLC coupled with UV detection, as described previously (27). Three nucleotide sugars were also analyzed by ion-pair, reversed-phase liquid chromatography electrospray ionization-MS/MS, as described previously (39).

ACKNOWLEDGMENTS. We thank our laboratory members, Drs. Robert S. Haltiwanger and Hideyuki Takeuchi (Stony Brook University, NY) and Drs. François Foulquier and Sandrine Duvet (Université des Sciences et Technologies de Lille, France) for fruitful discussions. We also thank Dr. Jianguo Gu (Tohoku Pharmaceutical University, Japan) for providing the plasmid. We greatly thank Drs. David Ron (University of Cambridge, United Kingdom) and Seiichi Oyadomari (University of Tokushima, Japan) for providing PERK$^{-/-}$ MEFs and helpful suggestions. This work was partially supported by grant-in-aids from the Ministry of Education, Culture, Sports, Science, and Technology of Japan (Grant 24770134 to Y.H. and Grant 25291030 to T.S.). H.H.F. was supported by Grant R01DK55615 and The Rocket Fund.

1. Aebi M, Bernasconi R, Clerc S, Molinari M (2010) N-glycan structures: Recognition and processing in the ER. *Trends Biochem Sci* 35(2):74–82.
2. Kelleher DJ, Gilmore R (2006) An evolving view of the eukaryotic oligosaccharyltransferase. *Glycobiology* 16(4):47R–62R.
3. Ruiz-Canada C, Kelleher DJ, Gilmore R (2009) Cotranslational and posttranslational N-glycosylation of polypeptides by distinct mammalian OST isoforms. *Cell* 136(2): 272–283.
4. Schwarz F, Aebi M (2011) Mechanisms and principles of N-linked protein glycosylation. *Curr Opin Struct Biol* 21(5):576–582.
5. Helenius J, et al. (2002) Translocation of lipid-linked oligosaccharides across the ER membrane requires Rft1 protein. *Nature* 415(6870):447–450.
6. Sanyal S, Menon AK (2009) Specific transbilayer translocation of dolichol-linked oligosaccharides by an endoplasmic reticulum flippase. *Proc Natl Acad Sci USA* 106(3): 767–772.
7. Fernandez F, et al. (2001) The CWH8 gene encodes a dolichyl pyrophosphate phosphatase with a luminally oriented active site in the endoplasmic reticulum of Saccharomyces cerevisiae. *J Biol Chem* 276(44):41455–41464.
8. Rush JS, Cho SK, Jiang S, Hofmann SL, Waechter CJ (2002) Identification and characterization of a cDNA encoding a dolichyl pyrophosphate phosphatase located in the endoplasmic reticulum of mammalian cells. *J Biol Chem* 277(47):45226–45234.
9. van Berkel MA, et al. (1999) The Saccharomyces cerevisiae CWH8 gene is required for full levels of dolichol-linked oligosaccharides in the endoplasmic reticulum and for efficient N-glycosylation. *Glycobiology* 9(3):243–253.
10. Freeze HH (2013) Understanding human glycosylation disorders: Biochemistry leads the charge. *J Biol Chem* 288(10):6936–6945.
11. Kelleher DJ, Karaoglu D, Mandon EC, Gilmore R (2003) Oligosaccharyltransferase isoforms that contain different catalytic STT3 subunits have distinct enzymatic properties. *Mol Cell* 12(1):101–111.
12. Breuer W, Bause E (1995) Oligosaccharyl transferase is a constitutive component of an oligomeric protein complex from pig liver endoplasmic reticulum. *Eur J Biochem* 228(3):689–696.
13. Peric D, et al. (2010) The compartmentalisation of phosphorylated free oligosaccharides in cells from a CDG Ig patient reveals a novel ER-to-cytosol translocation process. *PLoS ONE* 5(7):e11675.
14. Vleugels W, et al. (2011) Identification of phosphorylated oligosaccharides in cells of patients with a congenital disorders of glycosylation (CDG-I). *Biochimie* 93(5):823–833.
15. Baumann H, Jahreis GP (1983) Glucose starvation leads in rat hepatoma cells to partially N-glycosylated glycoproteins including alpha 1-acid glycoproteins. Identification by endoglycolytic digestions in polyacrylamide gels. *J Biol Chem* 258(6):3942–3949.
16. Turco SJ, Pickard JL (1982) Altered G-protein glycosylation in vesicular stomatitis virus-infected glucose-deprived baby hamster kidney cells. *J Biol Chem* 257(15):8674–8679.
17. Rearick JI, Chapman A, Kornfeld S (1981) Glucose starvation alters lipid-linked oligosaccharide biosynthesis in Chinese hamster ovary cells. *J Biol Chem* 256(12):6255–6261.
18. Gershman H, Robbins PW (1981) Transitory effects of glucose starvation on the synthesis of dolichol-linked oligosaccharides in mammalian cells. *J Biol Chem* 256(15):7774–7780.
19. Isono T (2011) O-GlcNAc-specific antibody CTD110.6 cross-reacts with N-GlcNAc2-modified proteins induced under glucose deprivation. *PLoS ONE* 6(4):e18959.
20. Anumula KR, Spiro RG (1983) Release of glucose-containing polymannose oligosaccharides during glycoprotein biosynthesis. Studies with thyroid microsomal enzymes and slices. *J Biol Chem* 258(24):15274–15282.
21. Gao N, Shang J, Lehrman MA (2005) Analysis of glycosylation in CDG-Ia fibroblasts by fluorophore-assisted carbohydrate electrophoresis: implications for extracellular glucose and intracellular mannose 6-phosphate. *J Biol Chem* 280(18):17901–17909.
22. Cacan R, Hoflack B, Verbert A (1980) Fate of oligosaccharide-lipid intermediates synthesized by resting rat-spleen lymphocytes. *Eur J Biochem* 106(2):473–479.
23. Suzuki T, et al. (2008) Dual-gradient high-performance liquid chromatography for identification of cytosolic high-mannose-type free glycans. *Anal Biochem* 381(2):224–232.
24. Pouysségur J, Shiu RP, Pastan I (1977) Induction of two transformation-sensitive membrane polypeptides in normal fibroblasts by a block in glycoprotein synthesis or glucose deprivation. *Cell* 11(4):941–947.
25. Scheuner D, et al. (2001) Translational control is required for the unfolded protein response and in vivo glucose homeostasis. *Mol Cell* 7(6):1165–1176.
26. Harding HP, Zhang Y, Bertolotti A, Zeng H, Ron D (2000) Perk is essential for translational regulation and cell survival during the unfolded protein response. *Mol Cell* 5(5):897–904.
27. Nakajima K, et al. (2010) Simultaneous determination of nucleotide sugars with ion-pair reversed-phase HPLC. *Glycobiology* 20(7):865–871.
28. DeRossi C, et al. (2006) Ablation of mouse phosphomannose isomerase (Mpi) causes mannose 6-phosphate accumulation, toxicity, and embryonic lethality. *J Biol Chem* 281(9):5916–5927.
29. Sharma V, Freeze HH (2011) Mannose efflux from the cells: A potential source of mannose in blood. *J Biol Chem* 286(12):10193–10200.
30. Fujita N, et al. (2008) The relative contribution of mannose salvage pathways to glycosylation in PMI-deficient mouse embryonic fibroblast cells. *FEBS J* 275(4):788–798.
31. Thiel C, et al. (2003) A new type of congenital disorders of glycosylation (CDG-Ii) provides new insights into the early steps of dolichol-linked oligosaccharide biosynthesis. *J Biol Chem* 278(25):22498–22505.
32. O'Reilly MK, Zhang G, Imperiali B (2006) In vitro evidence for the dual function of Alg2 and Alg11: essential mannosyltransferases in N-linked glycoprotein biosynthesis. *Biochemistry* 45(31):9593–9603.
33. Kämpf M, Absmanner B, Schwarz M, Lehle L (2009) Biochemical characterization and membrane topology of Alg2 from Saccharomyces cerevisiae as a bifunctional alpha1,3- and 1,6-mannosyltransferase involved in lipid-linked oligosaccharide biosynthesis. *J Biol Chem* 284(18):11900–11912.
34. Dennis JW, Nabi IR, Demetriou M (2009) Metabolism, cell surface organization, and disease. *Cell* 139(7):1229–1241.
35. Harding HP, et al. (2003) An integrated stress response regulates amino acid metabolism and resistance to oxidative stress. *Mol Cell* 11(3):619–633.
36. Hase S, Ikenaka T, Matsushima Y (1979) Analyses of oligosaccharides by tagging the reducing end with a fluorescent compound. I. Application to glycoproteins. *J Biochem* 85(4):989–994.
37. Hase S, Hara S, Matsushima Y (1979) Tagging of sugars with a fluorescent compound, 2-aminopyridine. *J Biochem* 85(1):217–220.
38. Hirayama H, Seino J, Kitajima T, Jigami Y, Suzuki T (2010) Free oligosaccharides to monitor glycoprotein endoplasmic reticulum-associated degradation in Saccharomyces cerevisiae. *J Biol Chem* 285(16):12390–12404.
39. Turnock DC, Ferguson MA (2007) Sugar nucleotide pools of Trypanosoma brucei, Trypanosoma cruzi, and Leishmania major. *Eukaryot Cell* 6(8):1450–1463.